Starter/Alternator Systems for HEV and Their Control: A Review

Ion. Boldea†

Abstract - Motor & generator operation at widely variable speeds is needed in various applications but hybrid and electric vehicle (HEV) stand out today, as quite a few companies are launching this year their mass production of HEVs. The quest for better starter-generators is far from ended, though. The present review paper unfolds a comparative critical evaluation of various starter-generators and their control for HEV. Induction, interior PM synchronous , transverse-flux PM synchronous , switched reluctance, together with claw-pole and biaxial excitation PM synchronous (BEGA) configurations with their control are all considered in system evaluations.

1. Introduction

Starter-alternators systems on board of electric and(or) hybrid electric vehicle (HEV) constitute an aggressive novel technology aimed at improving comfort, gas – mileage and environmental performance of road vehicles. The degree of electrification in a vehicle may be defined by the electric fraction [1] %E:

$$\%E = \frac{peak\ \text{electric power} \times 100}{\text{peak electric power} + \text{peak ICE power}} = \frac{P_{(el)} \times 100}{P_{(el)} + P_{(ICE)}}$$

For a standard ICE vehicle whose starter and alternator functions, only, are integrated %E<(5-10%). For a mild hybrid electric car %E goes to 10-15% at 42 Vdc. It may reach 60-70% for a full (strong) hybrid electric vehicle and it is 100% for a fully electric car. So there are basically 4 HEVs:

a. ICE vehicle with ISA (integrated starter alternator)
b. Mild HEV (with ISA)
c. Strong (full) HEV (with ISA)
d. Electric vehicle (with ISA)

Typical torque-speed for motoring and generator power/speed envelopes required from starter-alternators for cars are shown in Fig. 1. There are variations corresponding to car weight and acceleration to 100 km/h time specifications.

For buses the torque speed and power speed envelopes are about (or above) 2-3 times larger. The engine torque-speed envelopes in Fig. 1 refer to the torque and speed after eventual speed mechanical demultiplication.

A carefully chosen mechanical transmission may allow for less demanding electric torque/speed characteristics of a higher speed electric machine (up to 15000 rpm, in general).

Concerning the four main strategies of vehicle electrification we summarize here the world wide efforts so far:

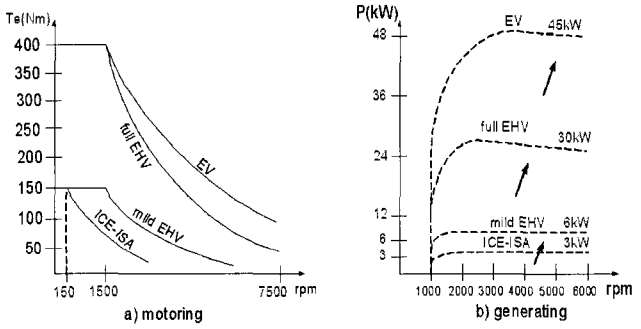

Fig. 1 Typical electric torque at engine crankshaft speed (for motoring) and electric power/speed envelope for small-medium size cars with various degrees of electrification

- For the ICE (standard) vehicles, the integrated starter-alternator has not reached the market but most probably will do so, soon, at 42 Vdc, for ICE starting torques at 150 Nm or more, with belt transmission (transmission ratio around 2.5(3):1) with maximum ISA speed of 15000 rpm and 3 kW of alternator delivered power from 1500 rpm engine speed onward. Full power electronics is required at least for starting (motoring). This performance, corroborated with cost constraints, may keep the claw-pole machine as a prime candidate if notable improvement on the machine in efficiency (about 70%) at reasonably higher costs, for the today's total machine volume, are feasible.
- For the mild HEV, a single model has reached the markets in 2002. It was again a claw-pole synchronous machine with electromagnetic excitation, 1/2.5 belt transmission, max electric motoring torque of 56 Nm

† Corresponding Author: University Politehnica of Timisoara, Romania(boldea@lselinux.utt.ro)
Received June 22, 2004 ; Accepted July 26, 2004

up to 300 rpm engine speed and 3.5 kW rated electric generating power, for a 42 Vdc battery [2]. The maximum electric machine speed is 15000 rpm. It claims a 15% gas consumption reduction for standard urban driving cycles. The ISA helps the vehicle in starting or it starts the car alone when the ICE is shut-off in traffic jams or at stop lights. It also provides for motoring some auxiliary load such as the air conditioner during idle engine stop. It also provides generating electric power for regenerative vehicle braking, battery recharge and all loads supplying on board. It uses a special, valve regulated lead- acid 42 Vdc battery of 20 Ah which weighs only 27 kg and is capable to deliver 6.1 kW for one second and allows for 3.5 kW for 5 seconds of regenerative braking operation power. For driving the auxiliaries it is capable to deliver 2.1 kW. For a mild hybrid pick-up truck (Chevrolet Silverado) at 14 kW electric power and 42 Vdc) [3], a 12% fuel economy is claimed.

- The full hybrid HEV has started to be mass produced in 1997 by Toyota (Prius) and Honda (Insight) and quite a few leading car manufacturers have announced the launching full hybrid SUVs since 2004 [3] (Volvo XC 90, Lexus RX 400H, Ford Escape hybrid). Toyota Prius boosts a 200 Vdc battery with a 200 V to 500 V d.c. – d.c. boost converter and inverters and a 50 kW powerful PMSM electric motor with acceleration to 100 Kmph in 10.5 seconds, about the same as Chrysler PT Cruiser with standard ICE. The fuel economy has improved to 4.28 l/100 km for a 1310 kg vehicle. The town mileage is even better: 3.92 l/100 km. Toyota Prius uses two electric machines in their hybrid synergy drive whose center is a central gear surrounded by planetary gears and a ring gear which is driven (or drives) by the main starter-alternator. The second starter-alternator works predominantly as a generator to supply the various electric loads but, when needed, participates in the optimum electric energy management on board. For SUVs the electric power level goes above 50 kW (65 KW in the Ford Escape Hybrid).
- Electric vehicles have been fabricated in small numbers for almost 100 years, but still the battery weight and costs prevented their advancement to mass production so far [4], though the traffic independence has reached even 150 km between two full battery chargings.

Note on main types of HEV: HEVs may be built in two main configurations: series and parallel (Fig. 2). In series HEV, the full power ICE drives the full power electric generator at rather constant (optimum versus load) speed. The generator supplies all the electric loads including the electric motor for full electric propulsion. Bidirectional power flow is secured through adequate static power converters. In series hybrids the electric power system is sized for the car total power/speed envelope but the ICE works at optimum speed, with good efficiency and (or) less pollution. In contrast, in parallel HEV, the ICE is undersized and so is the electric power system and they

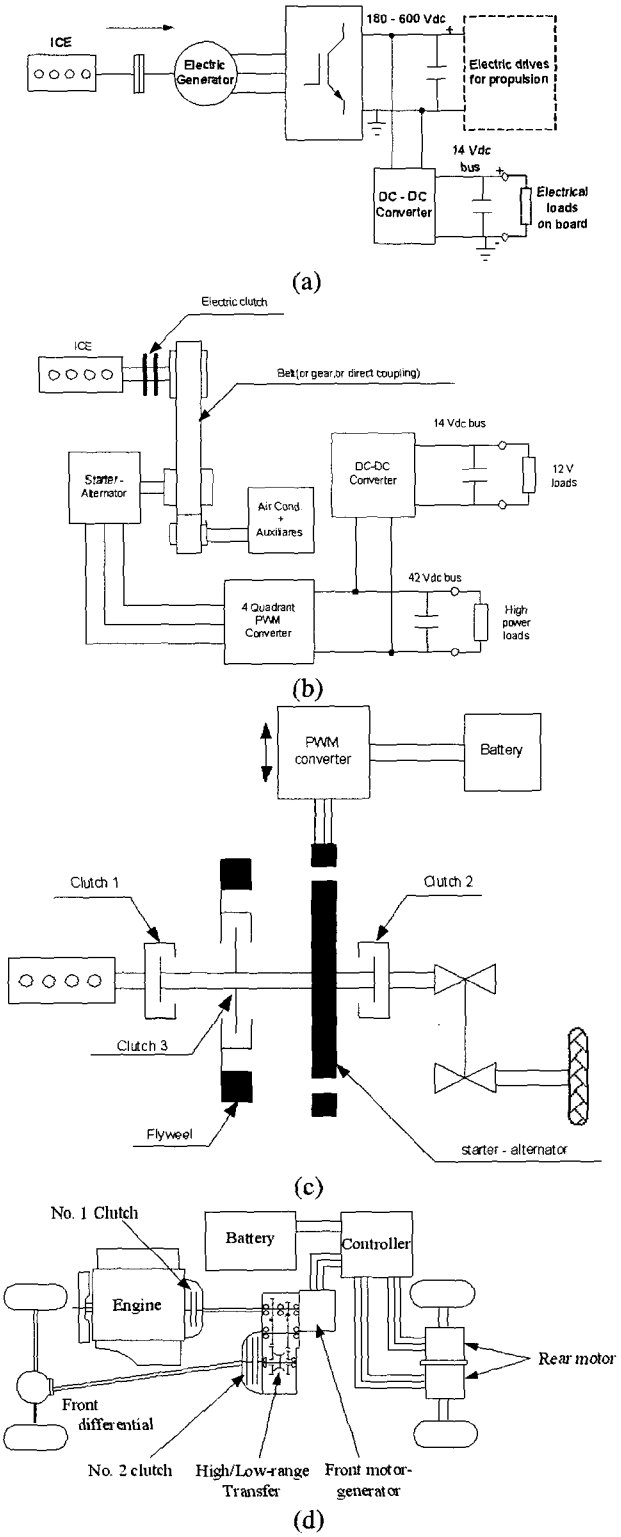

Fig. 2 Series & parallel HEVs : a) series b),c) parallel d) 4 wheel drive with electric rear wheel drive

work concurrently to propel the vehicle. In parallel HEVs the electric power system may be used also to transform a two wheel drive into a 4 wheel drive, with the electric propulsion being used to propel the rear wheels (Fig. 2.d.).

In series EHV the rotary ICE electric generator system may also be replaced by a linear oscillatory motion generator [5,6]. In what follows we will concentrate on integrated starter-generator systems (ISA) typical for ICE vehicles and for parallel hybrids.

Sample specifications and typical performance/costs for ISA systems

The following are considered as essential specifications for ISA:

- torque-speed envelope for motoring
- mechanical transmission ratio $K_e \geq 1$ between ISA and ICE speed
- power-speed envelope for generating
- battery voltage (minimum, maximum, rated)
- ISA & PWM inverter rated voltage (a voltage boost/buck dc.-dc. converter may be included between the battery and the PWM inverter to reduce the total power silicon costs and losses)
- Maximum ISA phase RSM current (for peak stall motoring torque)

There are also quite a few constraints on ISA system in terms of the shape of volume, over temperatures in critical points and system costs. In the design of ISA systems the ISA and the PWM converter (with and without d.c.-d.c. converter) the total losses per standard town driving cycle, for given specifications, should be constraint together with volume constraints, while the total system costs should be the main objective function. A comparison between various ISA system at 6 kW peak generating power at 42 Vdc, shown in Fig. 3 [7], indicates that at low voltage (42 Vdc) the converter cost is much larger then the ISA cost and thus only system optimization design is meaningful.

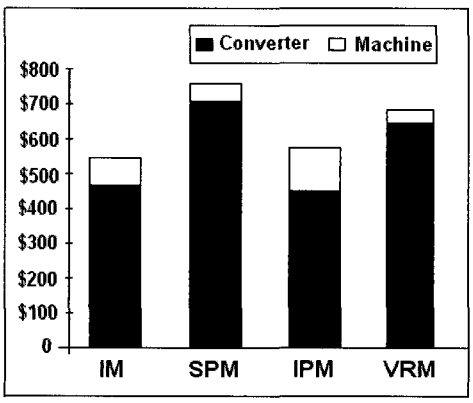

Fig. 3 ISA systems costs at 6 kW peak generating power [7]

The comparison tends to show that the interior PMSM machine (IPMSM) performs better. A similar conclusion is drawn in Ref. 8 for a peak power of 30 kW typical today for a mild hybrid. For larger powers, 75 kW, and lower speed vehicles (hybrid electric town buses) and rather large mechanical transmission ratio K_e (K_e >4) the excited synchronous motor/generator and the transverse flux PM synchronous machine (TF-PMSM) have been found very competitive in Ref 9. (Table 1).

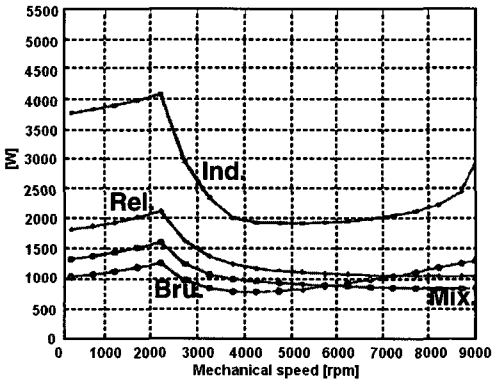

Fig. 4 Losses in 30 kW ISA systems [8]

Table 1 [9]

Feature / Machine	IM	SRM	HPSM
Volume(10^{-3}m)	53.2	44.0	37.6
Active Mass (kg)	272	147	106
Magnet Mass (kg)	-	-	2.7
Efficiency	0.900	0.930	0.932
Inverter Power (kVA)	396	984	254

Table 1 (continued)

Feature / Machine	RSM	PMSM	TFM
Volume (10^{-3}m)	35.0	38.9	22.3
Active Mass (kg)	79	71	73
Magnet Mass (kg)	4.7	7.0	11.5
Efficiency	0.941	0.949	0.976
Inverter Power (kVA)	361	385	455

Though Ref. 7,8,9 indicate as clear winners the IPMSM for wide constant power speed range (>4) (Fig.4) and TF-PMSM, for moderate constant power speed range ($\omega_{max}/\omega_b < 4$), in terms of losses and total system costs, the induction type ISA and the switched reluctance-ISA due to their robustness, for ($\omega_{max}/\omega_b < 4$) , should not be ruled out.

Finally, at least for ICE vehicles with ISA and mild HEV, rotor excited (eventually with PM and saliency rotors) should also be considered as, for $\omega_{max}/\omega_b < 8-10$, the peak kVA, and thus the converter and system costs, are reduced notably: a 3/1 belt transmission reduces the size of ISA which runs at up to 15000-18000 rpm . From this category we will treat the claw-pole machine synchronous

machine and the biaxial excitation generator for automobiles (BEGA) [10].

2. The Induction Isa

The induction-ISA may be used both for ICE vehicles to provide integrated starting & generating power and to supply the electrical loads on board, at powers bellow 6 kW and, for mild or full hybrid electric vehicles, when maximum powers may go as high as 50 kW, for cars. A typical such 42 Vdc, 9.5 peak kVA poly-V belted (K_e =3/1 speed ratio) ISA is shown in Fig. 5 [11]. The requirements in [11] were about 150 Nm (at engine shaft), for starting and up to 400 rpm and 3-4 kW at most speeds but at least 1kW at 6000 rpm engine speed (18000 rpm machine speed).

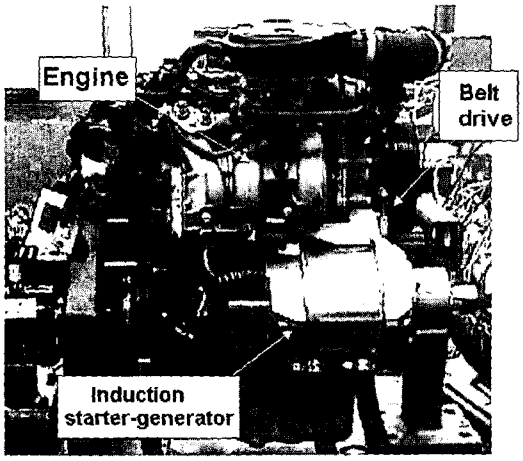

Fig. 5 Induction starter alternator[11]

The motor torque-speed envelope is shown in Fig. 6 and the generating power maximum capacity versus speed in Table 2.

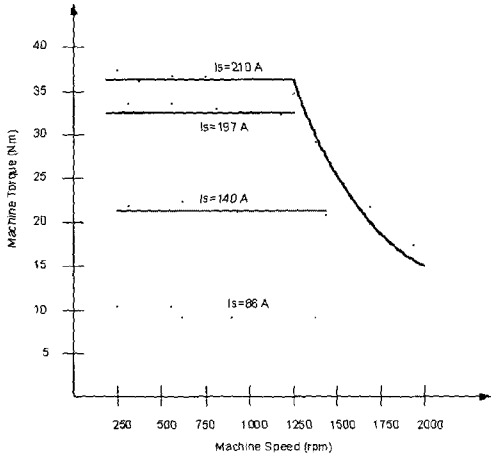

Fig. 6 Motor torque-speed [11]

Table 2 Maximum generated power versus engine speed [11]

Engine speed (rpm)	850	1500	2500	4000	4500	5000
Maximum power (kW)	3.945	3.775	3.750	1.850	1.800	1.500

The machine efficiency as generator at 1500 engine speed decreased from 94.5% at 0.750 kW dc, output to 85% at 3.750 KW dc output. It should be noted that at 6000 rpm no power could be delivered to the battery, [11].

Design aspects for high starting (motoring) torque and high maximum generator power wide speed range are given in what follows.

A practical design should realize the required starting torque and maximum generator power for wide speed range at lowest maximum current I_{Smax} as the dc voltage (eventually the maximum battery voltage) is given. To do so we start here with given, initial values of D_{is} (interior stator diameter), stack length l_{stack} (corresponding to 7-8 N/cm^2 peak rotor stress), airgap g = 0.7-1 mm and assume maximum torque per current at start and maximum torque per given voltage (flux) at maximum desired speed for which maximum power (motoring or generating) has to be provided. The machine has to be heavily saturated with airgap flux density B_g= 0.95-1.10 T, and the number of poles $2p$=8,10,12 in general, for higher torque density.

The vector (or DTFC) control for maximum torque per current may be approached with dq model currents $I_{ds}=I_{qs}=I_s$ (rms phase current) in rotor flux coordinates. For given stator current I_s^* (RMS phase value) [13].

$$T_e = \frac{3}{2} p (L_m - L_{rl}) I_{qs} I_{ds} \tag{1}$$

Consequently:

$$T_{e\max} = \frac{3}{2} p (L_{msat} - L_{rl}) I_{s\max}{}^2 \tag{2}$$

L_{msat} – rated magnetization inductance, L_{rl} – rotor leakage inductance, p - pole pairs. With

I_{smax} and T_{emax} given and $L_{rl}/L_{msat} = 0.1-0.2$, the magnetization inductance Lm may be found [12]:

$$L_{msat} = \frac{6(w_1 k_{w1}/a)^2 \tau l_{stack}}{\pi^2 g K_c (1+K_s)}; \quad \tau = \frac{\pi D_{is}}{2p} \tag{3}$$

K_s – saturation factor, K_c – Carter coefficient, w_1/a - turns per current path, a – current path count, k_{w1} – winding factor. With K_c=1.3-1.4 and (K_s=1.3-1.7) as given, the number of turns per current path w1/a is found and rounded

to an integer. Then the flux density condition in the airgap is checked:

$$B_g = \frac{u_0 3\sqrt{2}\left(w_1\left(I_{ds}/\sqrt{2}\right)k_{w1}/a\right)}{\pi g K_c (1+K_s)} = 0.95-1.05\ \text{T} \quad (4)$$

If $B_g > 1.10\ T$ then the FEM is used to check again. If still $B_g > 1.10\ T$ the stack length l_{stack} or (and) the stator interior diameter D_{is} have to be increased. FEM provides implicitely the value of $K_C(1+K_S)$. After a few iterations, where the size of the stator or (and) rotor slotting area are modified, the value of $K_C(1+K_S)$ converges also. Adjustment in the value of I_{ds} around $I_{s\max}$ (RMS per phase) will provide for the actual maximum value of stall torque per current in conditions of heavy magnetic saturation.

For the maximum power conditions at large speed at given (large speed) P_{ek}, ω_{rk}, verifications are done with the maximum torque per flux condition:

$$\Psi_{sk} = \frac{V_S(0.92-0.95)}{\omega_{rk}+(s\omega_1)_k}\ ; \qquad L_{sa} = L_{ma}+L_{sl};\quad L_{ra} = L_{ma}+L_{rl} \quad (5)$$

and

$$i_{dk} = \frac{\Psi_{sk}}{\sqrt{2}(L_{ma}+L_{sl})};\quad i_{qk} = \frac{\Psi_{sk}}{\sqrt{2}(L_{sl}+L_{rl})};\qquad (s\omega)_k = \frac{R_r}{L_{ra}}\cdot\frac{L_{sa}}{L_{sc}} \approx \frac{R_r}{L_{sc}} \quad (6)$$

L_{ma} – unsaturated value of magnetization inductance, L_{sl} – stator leakage inductance.

And the torque T_{ek} is :

$$T_{ek} = \frac{P_{ek}}{\omega_{rk}}p = \frac{3}{2}p(L_{ma}-L_{rl})\frac{\Psi_{sk}^{\ 2}}{2L_{sa}L_{sc}} \quad (7)$$

The voltage V_s (d- q model voltage) given:

$$V_s = V_{dc}\cdot\frac{2}{\pi}(0.92-0.96) \quad (8)$$

We may check from the above if the machine is capable to produce P_{ek} at ω_{rk}. If not, the number of turns per current path has to be reduced and thus the peak current (at given stall torque) increases also. And so is the inverter cost. Plus the battery might not be able to withstand it.

Note : A practical alternative solution to reduce peak current at stall and produce high power at large speed is to switch from star to delta connection at a certain speed as illustrated in Fig. 7.

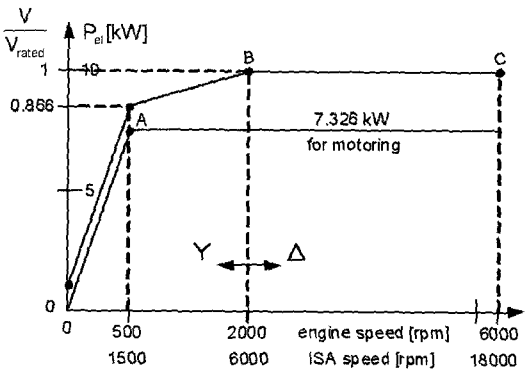

Fig. 7 Voltage for wide speed constant peak power motoring of an induction ISA with Y to Δ winding switching

What limits the power delivered by an induction ISA is the fact that, for maximum torque per flux, the flux in axis q and d (aligned with the rotor flux) are equal to each other. So it is too much flux for the torque produced, which makes the available voltage too small at high speeds.

On the other hand, the large value slip frequency $(s\omega_1)_k$ at P_{ek} leads to large rotor losses and to low power factor (around 0.707), at the low flux level attainable at high speed.

Even with copper bar cage rotor, the rotor losses are at least 50% of stator winding.

3. The Ipmsm-Isa

The interior PMSM machine with multiple flux barrier rotor, called also the PM-assisted Reluctance Synchronous Machine (PM-RSM) – Fig.8 – is credited with an unusually large constant power speed range [14] due to the possibility to cancel the flux linkage in axis q at a certain current , i_{qk}:

$$\Psi_q = L_q i_{qk} - \Psi_{PMq} = 0 \quad (9)$$

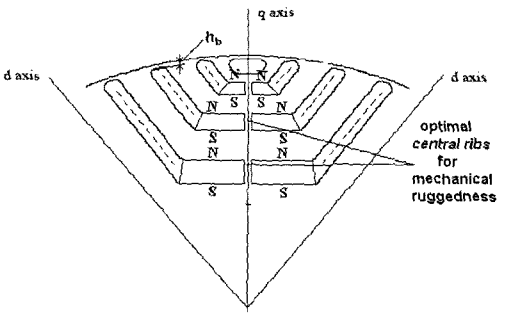

Fig. 8 IPMSM with multiple flux barrier rotor

As the machine has notable magnetic saliency, with $L_d/L_q>2.5\text{-}3$ even for heavily saturated conditions, the torque has now two components [14]:

$$T_e=\frac{3}{2}p\left(\Psi_d i_q-\Psi_q i_d\right)=\frac{3}{2}p\left[\Psi_{PMq}+\left(L_d-L_q\right)i_q\right]i_d \quad (10)$$

The stator flux (in the dq model) is:

$$\bar{\Psi}_S=L_d i_d+j\left(L_q i_q-\Psi_{PMq}\right) \quad (11)$$

The steady state equation in space phasor form is :

$$\bar{V}_S=R_S i_S+j\omega_1\bar{\Psi}_S \quad (12)$$

Let us notice that for $\Psi_q=0$ the stator flux d axis component $\Psi_d=L_d i_d$ interacts with the current q axis current component i_{qk} to produce torque. The vector diagram in Fig. 9b, for $\Psi_q=0$, shows also a very good power factor when the speed is high as the stator flux Ψ_{sk} is provided only along axis d (and id is small) if $\Psi_q=0$. For maximum torque at stall ($\omega_1=0$) the power factor is unity again by principle (Fig. 9a).

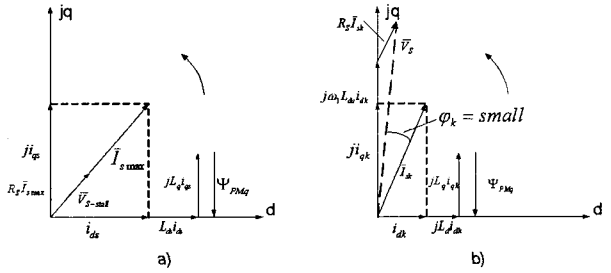

Fig. 9 The IPMSM vector diagram at zero q-axis flux
a) at zero speed and maximum torque
b) at maximum power and high speed

This simple property ($\Psi_q=0$) makes the IPMSM capable of large power-speed range. We should add that it also results into smaller peak current for same stall torque and *Pek*, ω_{ek} conditions, when compared with the IM or SRM.

In addition, the losses in the rotor core and PMs, due to stator space and time field harmonics, are small [15]. Here we are making use of the $\Psi_q=0$ conditions to design the IPM-SM for IGA applications.

For stall torque T_{emax}:

$$T_{e\max}=\frac{3}{2}p\Psi_{dsat}I_{qk}\ ;\ I_{qk}=\frac{\Psi_{PMq}}{L_{qm}+L_{sl}} \quad (13)$$

The PM flux Ψ_{PMq} is calculated based on a given percentage of emf E at max speed:

$$E_{\max}=(150-250)\%V_{Srated}=\omega_{r\max}\Psi_{PMq} \quad (14)$$

T_{emax} is produced under saturated conditions and for given initial stator bar diameter, D_{is}, and stack length, l_{stack}.

In contrast, at maximum power P_{ek}, ω_{rk} :

$$T_{ek}=\frac{P_{ek}p}{\omega_{rk}}=\frac{3}{2}p\Psi_{du}I_{qk} \quad (15)$$

But :

$$\Psi_{du}=\Psi_{sk}=(0.92-0.95)V_{dc}\frac{2}{\pi\omega_{rk}} \quad (16)$$

So from (15), with T_{ek}, p and Ψ_{du} known, I_{qk} is obtained Then, from (13), Ψ_{dsat} is obtained. Now we have to verify that Ψ_{dsat} corresponds to an axis d airgap flux density fundamental of $B_{gmax}=0.95\text{-}1.1$ T, for a value Ids calculated from the maximum current at peak stall torque I_{smax} (RSM, per phase):

$$I_{ds}=\sqrt{\left(\sqrt{2}I_{s\max}\right)^2-I_{qk}^{\ 2}} \quad (17)$$

Consequently :

$$L_{ds}=\Psi_{dsat}/I_{ds} \quad (18)$$

And thus the number of turns per current path is obtained from (3), for given K_S.

But:

$$L_{ds}=L_{sl}+L_{ms}K_{dm}\ ;\ K_{dm}=0.92-0.95 \quad (19)$$

K_{dm} – is the d axis magnetization inductance reduction coefficient due to the presence of flux barriers along q axis with $L_{sl}\approx(0.1-0.2)L_{sat}$, for $2p$=8,10,12.

Then, in (4) slightly modified:

$$T\ 0.95<B_{g\max}=\frac{u_0 3\sqrt{2}\left(w_1k_{w1}/a\right)\left(I_{ds}/\sqrt{2}\right)}{\pi g K_C\left(1+K_{sd}\right)}K_{dm}<1.1\ T \quad (20)$$

we check the peak airgap flux density.

For values of $K_S=K_{Sd}$=1.3-1.7, in general, condition (20) has to be fulfilled. Even if fulfilled analytically, FEM has to be used to check B_{gmax} again. If (20) is not met, the machine design has to be changed by modifying D_{is}, l_{stack}, the airgap g and stator slotting and rotor flux barrier area until convergence is met.

Finally the PM flux linkage for zero stator current is verified by FEM:

$$\Psi_{PMq} = \frac{2}{\pi} B_{g1PM} l_{stack} \cdot \left(\frac{w_1}{a}\right) k_{w1} \qquad (21)$$

where B_{1gPM} is the PM airgap flux linkage density fundamental. The above design rationale makes sure that the machine produces both T_{emax} at stall and P_{emax} at ω_{rPemax}, for limited emf at maximum speed for given maximum current I_{smax} and battery voltage.

Note: Accounting for saturation in the d axis magnetization inductance L_{dm} is feasible through analytical means. And so is the expression of L_{qm}, but still FEM verifications are required as very advanced magnetic saturation is implicit at stall peak torque. The saliency ratio under saturation conditions L_{dmsat}/L_{qmsat} is in the interval 3-5 at best in IPMSM-ISA for peak powers up to 50 kW and stall torque up to 400 Nm. The total saliency L_{dsat}/L_q~*2.5-4.0* under saturated conditions is very close to L_{sat}/L_{sc} of the corresponding induction machine with same stator and airgap. The main advantage of IPMSM stands in the possibility to cancel the flux in axis q due to the presence of PMs.

Control Of IPMS-ISA

A typical motion sensorless control system for an ISA, as adapted to IPMSM is shown in Fig. 10.

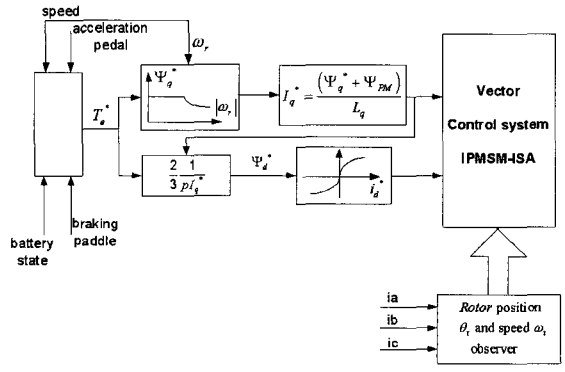

Fig. 10 Motion sensorless vector control of IPMSM-ISA

Though in generator mode the ISA delivers power, the latter may be "translated" into a certain (negative) torque, as speed is estimated anyway. The driver's intentions, manifested through the acceleration and braking paddles, are to be tempered by the optimum exploitation of battery energy processing and for protection and ride comfort. When the torque reference is small it is feasible to reduce I_q from I_{qk} and thus allow for a certain negative flux in axis q, especially at low speeds, in order to reduce further the losses in the machine.

A simple way to do it is to assign:

$$I_q = I_{qk} \frac{|T_e^*|}{T_{e\max}(\omega_r)} > 0 \qquad (22)$$

Now T_{emax} could be the maximum torque available from the machine as a function of speed ω_r. This way better energy conversion ratios at lower load are obtained.

To provide for nonhesitant starting from any rotor position, the initial rotor position has to be estimated , together with a reliable rotor position observer at low speeds (below 10 rpm).Signal injection rotor position estimators are used for the scope [16 - 19], Fig. 11.Above certain speed switching to an emf type position/speed estimator is operated.

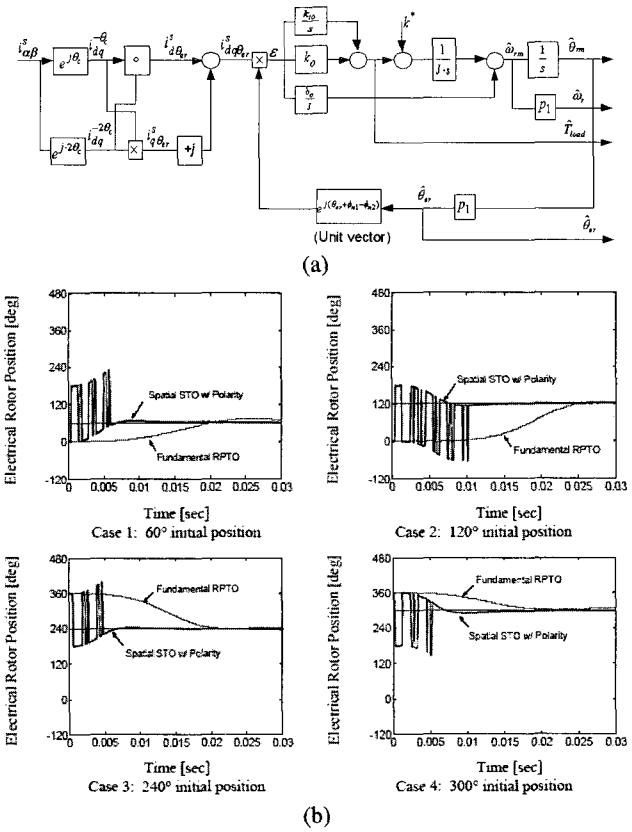

Fig. 11 Fundamental rotor – position and speed tracking observer [16]: (a) the observer; (b) initial position estimation test results.

Note: The induction – ISA does not need initial rotor position identification and DTFC sensorless control does not need signal injection to start non hesitantly and to work properly down to 3 rpm under moderately heavy load.

Our investigation here sustains previous findings that the IPMSM – ISA can produce a wider torque – speed envelope, for a smaller maximum current (25 % less) and same rotor voltage, for lower losses than the induction –

ISA with same stator. But both can produce a shear rotor stress (at stall) of 7 N/cm^2. However the IPMSM – ISA is capable of about 40 Nm/kW of losses while the induction ISA is capable of only 25 Nm/kW of losses at standstill.

4. The Switched Reluctance Machine

The switched reluctance machine has been thoroughly investigated for ISAs : both the machine and the controller (Fig. 12).

As for other ISAs, standstill maximum torque for motoring and maximum power delivered for generating at high speed are the main specifications that determine the machine and converter oversizing.

The power generation mode poses a severe problem in the sense that the excitation power to be built up in each phase each cycle may consume up to 30 % of the average maximum power available per energy per cycle.

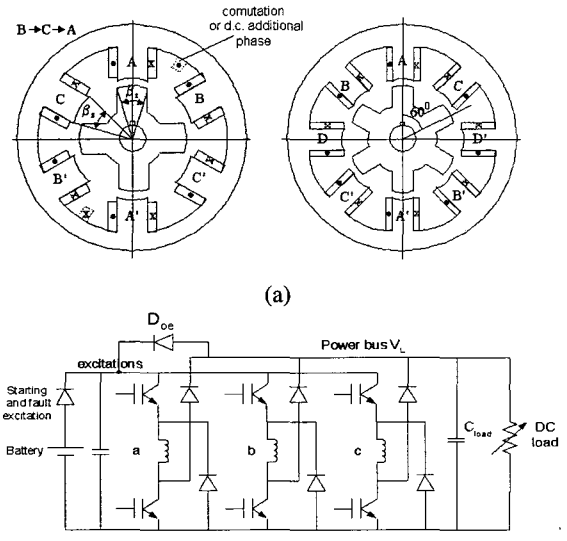

Fig. 12 The Switched Reluctance machine (SRM) ISA: (a) Three phase SRMs: (b) A typical converter with separate excitation and power bus and fault clearing [20].

Three typical phase current waveforms for generating mode are shown in Fig. 13, for same peak current value.

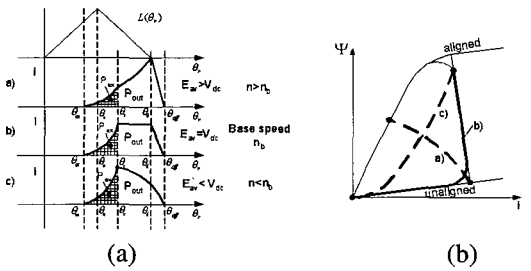

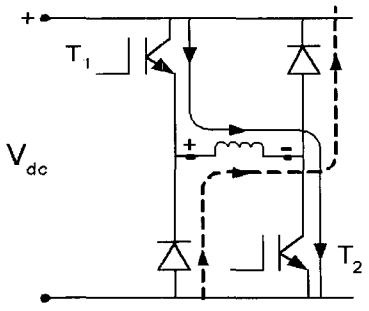

Fig. 13 SRM typical generating mode current waveforms a), their energy cycles, b) and pertinent phase-converter c) They are related to the emf/V_{dc} ratio at base speed :

$$emf = \frac{2\pi n_b}{\theta_w}(\Psi_{\max})_{current\ path} = \alpha_{pF} \cdot V_{dc} \tag{23}$$

θ_w - phase conducting angle $\theta_w = \theta_c - \theta_{on}$;

n_b - base speed (mechanical : rps)

α_{pF} is related to the machine equivalent "power factor". When large constant power speed range is required, $\alpha_{pF} < 1$ but, then, the number of turns per current path should be reduced and thus the peak current increases and heavy inverter oversizing is required. For $\alpha_{pF} > 1$ the constant power speed range is reduced but the number of turns per current path increases and thus the peak current decreases.

Starting the design with $\alpha_{pF} \approx 1$ at the base speed seems thus a good practice in order to reduce the number of designs before a good solution is found.

Anyway, for speeds $\omega_r > \omega_b$: $\alpha_{pF} > 1$ is typical while for $\omega_r < \omega_b$: $\alpha_{pF} < 1$ is characteristic.

The excitation penalty ε (Fig. 13) is :

$$\varepsilon = \frac{W_{exc}}{W_{out}} = \frac{\int_{\theta_{on}}^{\theta_c} i \cdot d\theta}{\int_{\theta_{on}}^{\theta_{off}} i \cdot d\theta} \tag{24}$$

The excitation penalty has conflicted effects on design.

Thus case *b* ($\alpha_{pF} = 1$) seems more effective in energy conversion. Maintaining case *b)* at speeds above ω_b (up to base speed) means to increase the output d.c. voltage of SRM in proportion to speed. To do so the converter should be size for this increased voltage and a step down converter is required to operate with a battery back-up source as typical for ISAs. A rather complete SRM – ISA control is

presented in Ref. 21.

Controlling the delivered generator power is feasible through the variation of turn on and turn off angles : θ_{on} and θ_{off} .

In general an excitation penalty of 30 – 40 % may lead to good energy conversion in the machine. An early soft turn off (Fig.13.a.c) may lead to additional delivered power in the generator mode.

The motor/generator mode control of SRM – ISA for wide speed range poses difficulties in implementing reliable position/speed observers from zero speed with initial position estimation for nonhesitant start, due to the nonsinusoidality of inductance variation with rotor speed and severe and variable magnetic saturation.

Recent progress through direct torque control of SRM [23 - 25] seems likely to produce more robust motion – sensorless control systems with fast torque response and capable to fully exploit the machine capabilities [26 - 27].

However with constant power speed ranges $\omega_{r\max}/\omega_b > 2-3$ it seems that the inverter current oversizing remains larger than for induction or IPMSM – ISAs.

5. The Transverse Flux Pm Machine (Tfm)

TFM in its interior PM (IPM) rotor configuration (Fig. 14) is credited with high torque density and high torque/losses

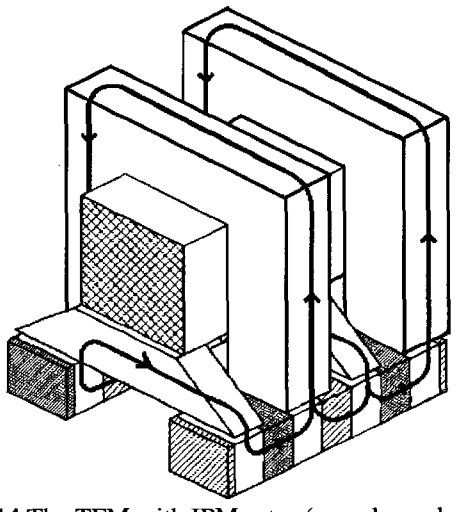

Fig. 14 The TFM with IPM rotor (one phase shown)

As a low saliency ratio ($L_d/L_q < 2$) machine, TFM is not endowed with large constant power speed range performance. It has, however, been proposed and tested on an 75 kW electric bus [9] where the constant power speed ratio is below 4:1. Plenty of oversizing of the machine ($f_t = 4\ N/cm^2$) and inverter was allowed, however.

The large number of poles leads to a high fundamental frequency at maximum speed which results into increased core losses and increased inverter switching losses. For highest torque density (7 N/cm^2 shear rotor stress in a 400 Nm machine) leads to a low power factor as only one half the PMs are working at any time (0.5).

The main obstacle in building TFM is the three dimensional flux path which implies, essentially, the using of magnetic powder in the stator magnetic core. A 30 % reduction in torque density, in comparison transverse (U shape) lamination stator core with silicon was calculated mainly due to the lower permeability (500 p.u.) of the magnetic powder maximum.

The rather compact TFM and high efficiency merits are paid for by the large peak KVA in the PWM converter required in a PMSM with low saliency IPM rotor. The TFM deserves renewed attention for ISA with up to 12 – 18 rotor poles to limit the fundamental frequency where a moderate constant power speed range ($\omega_{r\max}/\omega_b < 4$) is acceptable.

Other new configurations such as TFM with axial airgap [31] or Flux Reversal PM Machine (FRM) have been proposed also for the scope but so far none has reached the prototype stage for ISA and they all have somewhat similar problems with TFM.

NOTE: For enhanced performance automotive generators the rather standard PMSM with surface PM rotors and axial and radial airgap have been proposed, accompanied by a diode (or thyristor) rectifier and a dc – dc full converter. But, again, due to the inherent low constant power speed range (despite of good efficiency) the latter has not made it to prototyping for cars yet.

6. The Claw – Pole Starter – Alternator

The rotor claw pole synchronous (CP - SM) is still the single car alternator in use on ICE vehicles (Fig. 15).Though CP – SM has been built up to 5 kW and 18000 rpm as generator with diode rectifier and low power electronic excitation control, its exceptional power/volume ratio comes at a price of a total system efficiency of up to maximum of 65 % at maximum power and speed.

However, very recently, the CP – SM has been introduced as a belted starter – alternator, with full power electronics control (for motoring) on the first mild HEV [2]

It has a 56 Nm peak torque value, 3 kW rated (continuous) motoring and 3.5 kW generating, maximum speed 15000 rpm. The belt transmission ratio should be about 2.5. The peak electric torque at engine shaft, to start the ICE, is about 140 Nm.

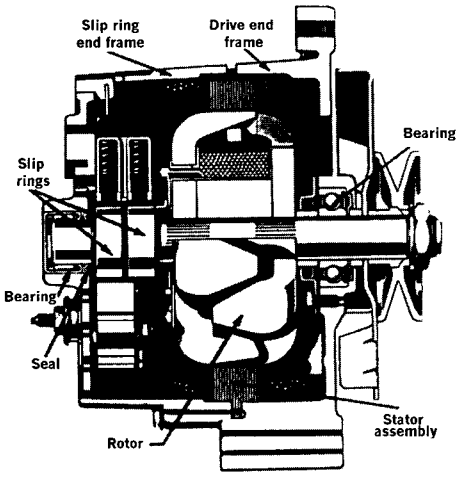

Fig. 15 Claw pole alternator

There are two main demerits of CP – SM for ISA:

- the rather low efficiency (high claw –pole eddy current, mechanical and stator copper losses);
- the presence of slip rings and brushes and the excitation low power rectifier + chopper control when for ICE starting (motoring), a full power PWM inverter to supply the stator windings is required for motoring ;

However, the excitation winding may prove very instrumental in producing the peak stall torque at 30 % less stator phase peak current, by controlling the machine with pure Iq stator current (Fig. 16).

The space vector steady-state equation of a synchronous machine in rotor coordinates are :

$$\begin{aligned} &\bar{I}_s \cdot R_s - \bar{V}_s = -j \cdot \omega_r \cdot \bar{\Psi}_s \\ &\Psi_d = \Psi_F = L_{dm} \cdot i_F^s \quad ; \quad i_{ds} = 0 \\ &\Psi_q = L_q \cdot i_q \quad ; \quad \bar{\Psi}_s = \Psi_d + j \cdot \Psi_q \\ &T_e = \frac{3}{2} p_1 \cdot L_{dm} \cdot i_F^* \cdot i_{qs} \end{aligned} \tag{25}$$

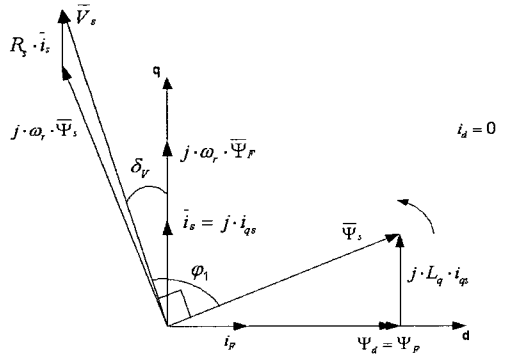

Fig. 16 The vector diagram of CP – SM at low speed

To change the torque sign (from generating to motoring) the sign of i_{qs} is changed.

At zero speed the frequency ω_r is zero and the current $\bar{i}_s = j \cdot i_{qs}$ is in phase with the stator voltage.

The reluctance torque ($L_d \neq L_q$) is zero as $i_{ds} = 0$ but, since $L_d / L_q < 1.5 - 1.6$, its production would not be very effective as it requires a large i_{ds} to produce it, witch, in turn, means large peak phase current in the stator. That is a larger PWM inverter size and costs.

The separate production of magnetic field through the field current releases the PWM inverter from a larger current sizing. This is a very good cost advantage.

The next problem is the wide high speed performance as a generator. The presence of the q axis flux $\Psi_q = L_q \cdot i_q$, even with pure i_q control and lower excitation current, still leaves too much flux in the machine for the produced torque for given voltage and high speed.

7. The Bega – Isa

In an attempt to reduce this flux a merger of IPMSM and CP – SM machine principles has been incorporated in BEGA – ISA [10], Fig. 17.

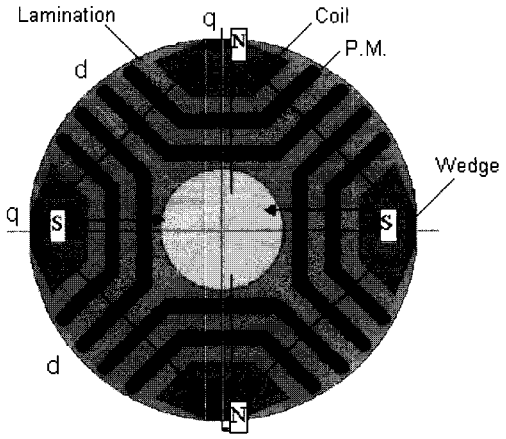

Fig. 17 BEGA – biaxial excitation generator for automobiles [10]

BEGA has a heteropolar excitation in axis d on a rotor with multiple flux barriers and IPMs in them, along axis q .

So the machine equations are :

$$\begin{aligned} &\bar{i}_s \cdot R_s - \bar{V}_s = -j \cdot \omega_r \cdot \bar{\Psi}_s \\ &\bar{\Psi}_s = \Psi_d + j \cdot \Psi_q \\ &\Psi_d = L_{md} \cdot i_F^s + L_d \cdot i_d \qquad \Psi_q = L_q \cdot i_q - \Psi_{PMq} \\ &T_e = \frac{3}{2} \cdot p \cdot [L_{dm} \cdot i_F^s \cdot i_q + \Psi_{PMq} \cdot i_d + (L_d - L_q) \cdot i_d \cdot i_q] \end{aligned} \tag{26}$$

In this case, for maximum torque versus speed envelope, the control may maintain :

$$i_q = \Psi_{PMq}/L_q \;\; ; \;\; \Psi_q = 0 \tag{27}$$

Now again $i_{ds} = 0$ and thus the torque becomes :

$$T_e = \frac{3}{2} \cdot p \cdot L_{dm} \cdot i_F^s \cdot i_{qs} \tag{28}$$

This time the PM flux is not used apparently to produce torque, but to simplify the control. The p.u. value of Ψ_{PMq} is small to limit the emf at maximum speed for a wide constant power speed range, as required, from ISA.

To change the torque sign, the sign of field current it has to be changed (a four quadrant chopper is needed).Working with full flux in axis d , but produced solely by the field current, the machine is going to produce its maximum torque for minimum stator current and minimum stator flux. This latter attribute is very useful to increase maximum delivered power as the speed increases, because $\Psi_q = 0$ (Fig. 18).

Below maximum torque (power)/speed envelope (partial load) the q axis current may be reduced as already shown in the paragraph on IPMSM.

It is evident that BEGA, in principle, can produce same torque at same stator current at less flux ($\Psi_q = 0$) than the CP – SM. A large constant power speed range is obtained, but a four quadrant chopper is required as the sign of field current changes the torque sign.

The question arias if BEGA may produce the same torque density as the CP – SM. It may, but at same number of poles when, in addition, it lacks the rotor rather large claw pole eddy current losses. However the heteropolar excitation power is minimum, with a large number of poles, for the ring – shape single excitation coil. With 16 poles, and same airgap flux density the total losses in the excitation winding of BEGA would be at least four times higher than for the CP – SM. For a typical 3 kW motor/generator rated power and 16 poles it would mean about 400 W.

Now we have to trade these larger excitation losses of BEGA for claw – pole eddy current losses of the CP – SM. As at high speeds, anyway i_F^s is reduced, only at low speeds excitation losses are important but the four quadrant chopper has to be designed for this maximum excitation power.

A compromise may be reached if the rotor of the CP – SM is "transformed" into BEGA (Fig. 19).

Basically the stack length is added two end parts, insulated magnetically from the central stator core. The claw poles are shaped (and a little prolonged axially) to hold also PMs along axis q as for BEGA (radially magnetized). The emf (of PM) is limited for maximum speed again.

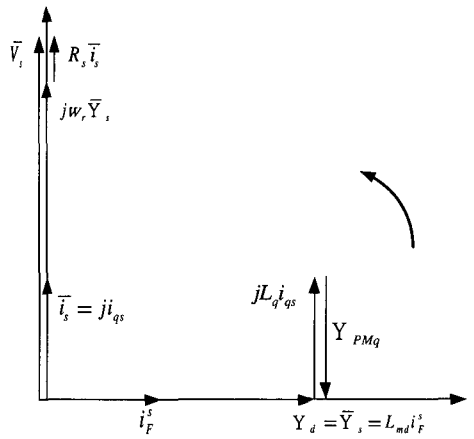

Fig. 18 BEGA vector diagram for motoring at $\Psi_q = 0$ and $i_d = 0$

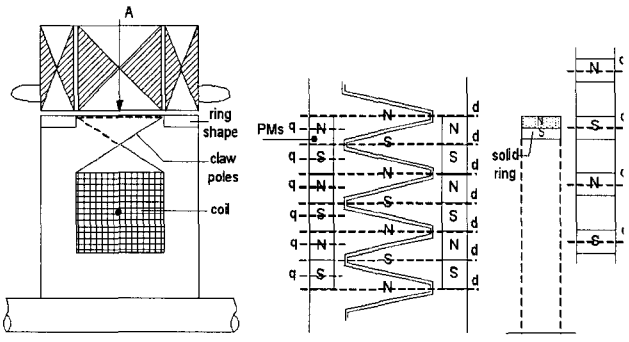

Fig. 19 The claw-pole rotor biaxial excitation generator/ motor for automobiles (CP – BEGA):(a) Longitudinal cross section ; (b) Radial unfolded view; (c) PMs between claws.

As we can see the two rotor sections are complementary and the machine magnetization inductances, L_{dm} and L_{qm} have two components :

$$\begin{aligned} L_{dm} &= L_{dm}^{CP} + L_{dm}^{PM} \\ L_{qm} &= L_{qm}^{CP} + L_{qm}^{PM} \end{aligned} \tag{29}$$

To make full use of the rotor (and stator) core for peak stall torque, now we have to allow some i_d to take advantage of the PM and reluctance torque (26). When $i_d = 0$ only the claw – pole segments of rotor (and stator) are active but still all stator winding losses are present.

This is what we meant by the compromise in building BEGA with a claw pole rotor.

It may be also worth considering to place the PMs in axis q but between the claw poles sticked to a solid magnetic ring placed below the claws, above the excitation coil (Fig. 19.c). This solid ring may act also as a d –axis damper winding.

The stator stack and rotor remain as in standard CP – SM but the contribution of the PMs tends to be smaller (thin magnets/pole), so better PMs might be needed.

The control of CP – SM or BEGA is similar to that of a SM with excitation (Fig. 20).

An additional regulator may be placed along i_q channel to make sure that $\Psi_q^* = 0$ when this is needed.

If motion sensorless is required, than rotor position and speed ($\hat{\theta}_r, \hat{\omega}_r$) have to be estimated as well.

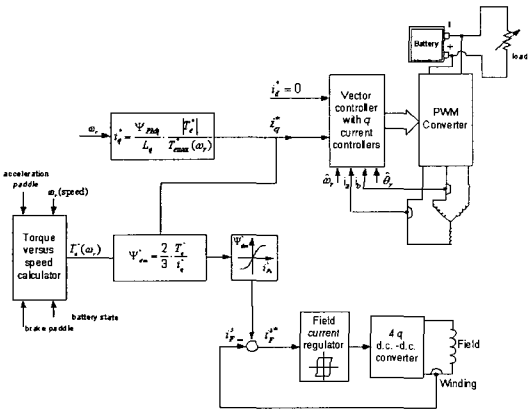

Fig. 20 Vector control of CP – SM and BEGA with $i_d = 0$ and $\Psi_q^* = 0$ for the torque/speed envelope.

8. Conclusion

- Integrated stator – alternators (ISAs) systems for hybrid vehicles have reached the markets in quite a few configurations ;
- ISAs are characterized by a wide torque/speed envelope for motoring and a wide power/speed envelope for generating at given battery d.c. voltage
- Though induction, IPM synchronous, transverse – flux PM synchronous, flux reversal, or other hybrid rotor (BEGA) machines have been proposed for ISA it seems that the IPMSM (with zero q axis flux control) offers the widest torque(power)/speed envelope in the same stator ;
- The claw pole starter/alternator is shown to fare well but only in its biaxial excitation (excitation + PM) – BEGA configuration it can operate at zero q axis flux and thus offer largest power/speed envelope ;also it boast minimum stator current for given stall torque, as the field in the machine is produced by the excitation current and $i_d = 0$;

The quest for better ISAs is far from ended (see Ref. 32 – 35 for more on the subject).

References

[1] J.M. Miller, V.R. Stefanovic, D. Kak, D. Pelergus, "Progresses For Starter – Alternator Systems In Automotive Applications", Record of EPE – PEMC – 2002, Dubrovnik & Cavtat, Croatia .

[2] T. Teratani et al , "Development Of Toyota Mild Hybrid System (THM - M) With 42 V Power Net", Record of IEEE – IEMDC – 2003, Vol 1, pp. 3 – 9.

[3] J. Voelker, "Top 10 Tech Cars : Here Come The Hybrids", *IEEE Spectrum*, March 2004, pp. 20 – 27.

[4] I. Husain, "Electric And Hybrid Vehicles", book, CRC Press, Florida, 2003.

[5] W. Cawthorne, P. Famouri, N. Clark, "Integrated Design Of Linear Alternator/Engine System For HEV Auxiliary Unit ", Record of IEEE – IEMDC – 2001.

[6] E.C. Losic, T.M. Lindback, W.M. Arshad, P. Telin, E. Nordlund, "Application Of Free – Piston Generator In A Series Hybrid Vehicle", Record of LDIA – 2003, Birmingan, UK, pp. 541 – 544.

[7] E.C. Lovelace, T.M. Jahns , J.L. Kirtley, J.H. Lang, "An Interior PM Starter Alternator For Automotive Applications ", Record of ICEM – 1998, Instambul, Vol. 3, pp. 1802 – 1808.

[8] A. Vaggati, A. Fratta, P. Gagliehni, G. Franchi, F. Villata, "Comparison Of A.C. Motor Based Drives For Electric Vehicle Application", Record of PCIM – 1999, Europe, Vol. IE, pp. 173 – 180.

[9] A. Lange, W.R. Canders, F. Laube, N. Mosebach, "Comparisons of Different Drive Systems for A 75 KW Electrical Vehicle", Record of ICEM – 2000, Espoo, Finland.

[10] S. Scridon, I. Boldea, I. Tutelea, F. Blaabjerg, "BEGA – Biaxial Excitation Generator For Automobiles. Full Characterization And Testing", Record of IEEE – IAS – 2004 Meeting.

[11] S. Chen, B. Lequensne, R.R. Henry, Y. Xuo, J. Ronning, "Design And Testing Of Belt – Driven Induction Starter - Generator", IEEE Trans., Vol. IA – 38, no. 6, 2002, pp. 1525 – 1532.

[12] I. Boldea, S.A. Nasar, *"Induction Machine Handbook", book*, CRC Press, Florida, 2001, pp.130

[13] I. Boldea, S.A. Nasar, *"Electric Drives", book*, CRC Press, 1999.

[14] I. Boldea, *"Reluctance Synchronous Machine And Drives", book*, Oxford University Press, 1996

[15] I. Boldea, L. Tutelea, C. I. Pitic, "Characterization Of

PM Assisted Reluctance Synchronous Motor/ Generator (PM-RSM) For a Mild Hybrid Vehicle", IEEE Trans. Vol. IA-40, no2, 2004, pp. 492 – 498.

[16] H. Kim, K. K. Huh, H. Harke, J. Wai, R. D. Lorenz, T. Jahns, "Initial Rotor Position Estimation For an Integrated Starter-Alternator IPMSM", Record of EPE-2003, Tolouse, France.

[17] M. Schroedl, "Sensorless Control of ac. Machines at Low Speed And Standstill Based On The INFORM Method", Record of IEEE-IAS, 1996, vol.1, pp. 270-277

[18] A. Consoli, G. Scarcella, A. Fratta, "Sensorless Control of PM Synchronous Motors At Zero Speed", Record of IEEE-IAS-1999, vol. 2, pp.1033-1040.

[19] Y. Yeong, R. D. Lorenz, T. M. Jahns, S. K. Sul, "Initial Rotor Position Estimation of IPMSM Using Carrier Frequency Injection Methods", Record of IEEE-IEMDC, 2003, Vol. 2, pp. 1218-1223.

[20] A. V. Radun , C. A. Ferreira, E. Richter, "Two Channel Switched Reluctance Starter-Generator Results", *IEEE Trans.* Vol. IA-34, no 5, 1998, pp. 1026-1034

[21] H. Baush, A. Grief, K. Kanelis, A. Milke, "Torque Control Of Battery Supplied Switched Reluctance Drives For Electric Vehicle", Record of ICEM-1998, Istambul, Vol 1, pp.229-234

[22] R. B. Inderka, R. W. De. Doncker, "Simple Average Torque Estimation for Control Of SRMs", Record of EPE-PEMC, 2000, Kosice, Vol. 5, pp. 176-181

[23] M. S. Islam, M. N. Anwar, I. Hussain, "A Sensorless Wide-Speed Range RSM Drive With Optimally Designed Critical Rotor Angles", Record of IEEE-IAS, 2000, Rome

[24] K. M. Rahman, S. E. Schultz, "High Performance Fully Digital Switched Reluctance Motor Controller For Vehicle Propulsion", IEEE Trans. Vol. IA-38, no 4, 2002, pp. 1062-1071

[25] R. B. Inderka, M., R. De. Doncker, "Control Of Switched Reluctance Drives For Electric Vehicle Applications", IEEE Trans. Vol. IE-49, no 1, 2002, pp. 48-53

[26] M. Eshani, B. Fahimi, "Elimination Of Position Sensor In Switched Reluctance Motor Drives: State Of The Art And Future Trends", IEEE Trans. Vol. IE-49, no 1, 2002, pp. 15-27

[27] T. J. E. Miller, "Optimal Design Of Switched Reluctance Motors", IEEE Trans. Vol. IE-49, no 1, 2002, pp.15-27

[28] H. Weh, M. May, "Achievable Force Densities With PM Excited Machines In New Configurations", Record of ICEM-1986, Munchen, Vol 3, pp. 1107-1011

[29] G. Hennenberger, I. A. Viorel, "Variable Reluctance Electrical Machines", book, Shaker Verlag, Aachen, 2001, chapter 6

[30] A. Njeh, A. Masmoudi, A. El-Antably, "3D-FEM based Investigation of Cogging Torque of a Transverse Flux PM Machine", Record of IEEE-IEMDC-2003, Vol.1, pp. 319-324

[31] J. Luo, S. Huang , S. Chen, T. A. Lipo, "Design and Experiments of a Novel Axial Circumpherential Current PM (AFCC0) Machine with Radial Airgap", Record of IEEE IAS-2001 Annual Meeting

[32] I. Boldea, "Automotive Electric Generator Systems – a review", Record of Electromotion 1999 Symposium, Patras, Greece.

[33] W. Lee, M. Sunwoo, "Vehicle Electric Power Simulator for Optimizing the Electric Charging System", International Journal of Automotive Engineering, Vol. 2, no 4, 2001, pp. 157-164

[34] T, Jahns, "Component Requirement for Wide Constant Power Operation of IPMSM Drives", Record of IEEE-IAS, 2000, Rome

[35] W. L. Soong, M. Ertrugrul, "Field Weakening Performance of IPMSM", Record of IEEE-IAS-2000, Rome.

Prof. Ion Boldea: IEEE Fellow.

He received his M.S. and Ph.D. degrees in 1967, respectively, 1973, from the University Politehnica (Enrollment: 11,000, all in Engineering) of Timisoara, Romania where he is a Full Professor. He spent about 5 years as Visiting Professor, Electrical Engineering in USA (in Kentucky and Oregon) since 1973 when he was a Senior Fullbright Scholar for 10 months. He was a Visiting Professor in UK at UMIST and Glasgow University for a few times. He worked and published extensively (above 100 publications in USA and UK) on Linear and Rotary Electric Machines, MAGLEVS and their control via Power Electronics. He also coauthored 13 books in USA and UK. Amongst them, five, coauthored with Prof. S.A.Nasar of University of Kentucky, are dedicated to linear motion machines and their control(in 1976, 1985, 1987, 1997, 2001).The last two books on linear machines are: (i) I. Boldea, and S.A. Nasar "Linear electric actuators and generators", Cambridge University Press, 1997; (ii) I. Boldea and S.A. Nasar "Linear motion electromagnetic devices", Taylor and Francis, 2001. The last two books on rotary electric machines and their control are: (i) I. Boldea and S.A. Nasar "Electric Drives" with attached CD interactive version, CRC Press, Florida, USA, 1998; (ii) I. Boldea and S.A. Nasar "Induction Machine Handbook"-950pp, CRC Press, 2001. Prof. I. Boldea is a member of IEEE-IAS, IDC and EMC commitees, Associate Editor of the EPCS Journal(owned by Taylor and Francis), Director and founder since 2001 of the Internet -only International "Journal of Electrical Engineering" -www.jee.ro- and Cochairman of Inter-national Conference OPTIM-1996, 1998, 2000, 2002, 2004-www.optim.8m. com- technically sponsored by IEEE-IAS. Prof. I. Boldea has been consulting , lecturing, giving keynote addresses and holding intensive courses in USA, Europe and Asia for the last 15 years .